Mineralogical Magazine, October 2013, Vol. 77(7), pp. 2931–2939

Oxyplumboroméite, $Pb_2Sb_2O_7$, a new mineral species of the pyrochlore supergroup from Harstigen mine, Värmland, Sweden

U. Hålenius[1,*] and F. Bosi[2,3]

[1] Department of Geosciences, Swedish Museum of Natural History, Box 50007, SE-10405 Stockholm, Sweden
[2] Dipartimento di Scienze della Terra, Sapienza Università di Roma, P. le A. Moro 5, I-00185 Rome, Italy
[3] CNR-IGG Istituto di Geoscienze e Georisorse, Sede di Roma, P. le A. Moro, 5, I-00185 Roma, Italy

[*Received 11 July 2013; Accepted 12 August 2013; Associate Editor: A. Christy*]

ABSTRACT

Oxyplumboroméite, $Pb_2Sb_2O_7$, is a new mineral of the roméite group of the pyrochlore supergroup (IMA 2013-042). It is found together with calcite and leucophoenicite in fissure fillings in tephroite skarn at the Harstigen mine, Värmland, Sweden. The mineral occurs as yellow to brownish yellow rounded grains or imperfect octahedra. Oxyplumboroméite has a Mohs hardness of ~5, a calculated density of 6.732 g/cm^3 and is isotropic with a calculated refractive index of 2.061. Oxyplumboroméite is cubic, space group $Fd\bar{3}m$, with the unit-cell parameters a = 10.3783(6) Å, V = 1117.84(11) Å^3 and Z = 8. The strongest five X-ray powder-diffraction lines [d in Å(I)(hkl)] are: 2.9915(100)(222), 2.5928(32)(400), 1.8332(48)(440), 1.5638(38)(622) and 1.1900(12)(662). The crystal structure of oxyplumboroméite was refined to an $R1$ index of 3.02% using 160 unique reflections collected with Mo$K\alpha$ radiation. Electron microprobe analyses in combination with crystal-structure refinement, infrared, Mössbauer and electronic absorption spectroscopy resulted in the empirical formula $^{A}(Pb_{0.92}Ca_{0.87}Mn_{0.09}Sr_{0.01}Na_{0.05})_{\Sigma 1.93}{}^{B}(Sb_{1.73}Fe^{3+}_{0.27})_{\Sigma 2.00}{}^{X+Y}[O_{6.64}(OH)_{0.03}]_{\Sigma 6.67}$. Oxyplumboroméite is the Pb analogue of oxycalcioroméite, ideally $Ca_2Sb_2O_7$.

Keywords: oxyplumboroméite, pyrochlore supergroup, roméite group, new mineral, crystal structure, Mössbauer spectroscopy, Harstigen, Sweden.

Introduction

The minerals of the pyrochlore supergroup are cubic and they crystallize in space group $Fd\bar{3}m$. Their general formula is $\mathbf{A}_{2-m}\ \mathbf{B}_2\ \mathbf{X}_{6-w}\ \mathbf{Y}_{1-n}$, in which **A** represents a large [8]-coordinated cation (e.g. Na, Ca, Ag, Mn, Sr, Ba, Fe^{2+}, Pb, Sn^{2+}, Sb^{3+}, Bi^{3+}, Y, *REE*, Sc, U, Th), a vacancy (□) or H_2O. **B** is a [6]-coordinated cation, as, e.g. Ta, Nb, Ti, Sb^{5+}, W or less commonly V^{5+}, Sn^{4+}, Zr, Hf, Fe^{3+}, Mg, Al and Si. **X** typically is O^{2-}, but can also be minor $(OH)^-$ and F^-. **Y** is an anion (OH^-, F^-, O^{2-}), but can also be a vacancy, H_2O, or a very large monovalent cation (e.g. K, Cs, Rb). Antimony is the dominant M^{5+} cation at the B site in minerals of the roméite group of the pyrochlore supergroup.

The recently published report on the pyrochlore supergroup (Atencio *et al*., 2010), amended by the Commission on New Minerals, Nomenclature and Classification (CNMNC) of the International Mineralogical Association (IMA) and the clarification of the status of species in the pyrochlore supergroup (Christy and Atencio, 2013) listed one approved roméite group mineral, oxycalcioroméite, ideally $Ca_2Sb_2O_7$, (Biagioni and Orlandi, 2012) and one transferred species, hydroxycalcioroméite = "lewisite", $(Ca,\#)_2Sb_2O_6OH$ (Hussak and Prior, 1895), where # denotes substituents and

* E-mail: ulf.halenius@nrm.se
DOI: 10.1180/minmag.2013.077.7.04

vacancies that bring the formula to electroneutrality. In addition, a number of possible new species were suggested on the basis of partial characterizations. Among these, "fluornatroroméite" was identified on the basis of a published structure refinement (Matsubara *et al*., 1996) and "fluorcalcioroméite" and "oxyplumboroméite" were suggested on the basis of published electron microprobe analyses by Brugger *et al*. (1997) and Christy and Gatedal (2005), respectively. Fluorcalcioroméite has subsequently been fully characterized and accepted as a valid mineral species by CNMNC (Atencio *et al*., 2013). Additionally, Atencio *et al*. (2010) and Christy and Atencio (2013) considered a number of existing mineral species in the roméite group to be questionable and needing further examination. Among these were bismutostibiconite (Walenta, 1983) and the grandfathered minerals partzite, stetefeldtite, stibiconite, monimolite and bindheimite. Bismutostibiconite, partzite, (Arents, 1867), stetefeldtite (Riotte, 1867) and stibiconite (Beudant, 1837) were considered likely equivalents of the possible new species "bismutoroméite", "cuproroméite", "argentoroméite" and "stibioroméite", respectively. Monimolite and bindheimite were believed to be identical to a possible new species "oxyplumboroméite". However, although questionable, the species bindheimite and monimolite have not been formally discredited and so far it has not been established that they are identical to the possible new species, oxyplumboroméite (Atencio *et al*., 2000).

In the present work we have examined a specimen from the original Igelström (1865) collection of monimolite from the Harstigen mine at Pajsberg, Värmland, Sweden. This and two others of Igelström′s monimolite specimens from this locality were donated in the late 19th century to the Swedish Museum of Natural History. The one chosen (collection number g22779) for the present work fits the original species description made by Igelström (1865) best. However, there exists no documentation to prove that it is identical to the actual specimen(s) on which he based his publication. The monimolite specimen examined demonstrates that it is indeed identical to oxyplumboroméite as suggested in the recently amended IMA report on the nomenclature of the pyrochlore supergroup (Atencio *et al*., 2010).

The new species oxyplumboroméite has been approved by the CNMNC (proposal IMA 2013-042). As a consequence of this, "monimolite" should be discredited as a valid mineral name. The holotype specimen of oxyplumboroméite is deposited in the collections of the Swedish Museum of Natural History, Stockholm, Sweden under catalogue number g22779. The formal description of the species is presented here including characterization of its physical, chemical and structural properties by means of electron microprobe, single crystal and powder X-ray diffraction, single-crystal Fourier Transform Infrared (FTIR) and electronic absorption spectroscopy, and powder ^{57}Fe Mössbauer techniques.

Occurrence, appearance, physical and optical properties

In the examined holotype specimen from the Harstigen iron-manganese mine, Pajsberg, Värmland, Central Sweden (59.60ºN, 14.23ºE), oxyplumboroméite occurs in aggregates of rounded grains or imperfect octahedral crystals, with partially developed {111} forms, together with calcite and leucophoenicite in fissure fillings ($\leqslant$2 cm) in tephroite skarn. The aggregates may reach 2 mm in size, but individual crystals of oxyplumboroméite are <0.4 mm across. The crystals are yellow to brownish yellow (Fig. 1) with a straw-yellow streak. They are brittle and show uneven fracture. Oxyplumboroméite has a Mohs hardness of ~5 and a calculated density of 6.732 g/cm^3. It is isotropic and a calculated refractive index, based on its empirical formula and the Gladstone-Dale relationship (Mandarino, 1979 and 1981), n = 2.061. Table 1 compares

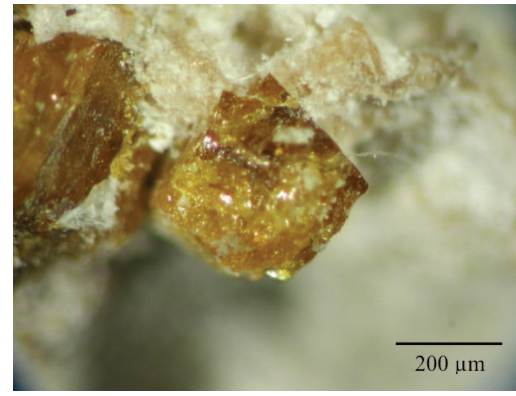

FIG. 1. Photomicrograph showing an imperfect octahedron of brownish yellow oxyplumboroméite on a matrix of calcite (white) and leucophoenicite (pink).

TABLE 1. Comparative data for oxyplumboroméite, oxycalcioroméite and fluorcalcoroméite.

Mineral	Oxyplumboroméite	Oxycalcioroméite	Fluorcalcioroméite
Formula	$Pb_2Sb_2O_7$	$Ca_2Sb_2O_7$	$(Ca_{1.5}\square_{0.5})Sb_2O_6F$
Space group	$Fd\bar{3}m$	$Fd\bar{3}m$	$Fd\bar{3}m$
a (Å)	10.3783	10.3042	10.2987
Z	8	8	8
Strong lines in the powder XRD pattern		5.93 (32)	5.934 (81)
		3.105 (24)	3.102 (20)
d (Å), I (%)	2.9915 (100)	2.977 (100)	2.969(100)
	2.5928 (32)	2.576 (24)	2.572 (6)
		1.984 (8)	1.979 (7)
	1.8332 (48)	1.824 (45)	1.818 (8)
	1.5638 (38)	1.556 (34)	1.551 (15)
	1.1900 (12)		
Refractive index	2.061 calculated	1.9625 calculated	1.826 calculated
Density (g/cm^3)	6.732 calculated	5.442 calculated	5.113 calculated
References	This work	Biagioni and Orlandi (2012)	Atencio *et al*. (2013)

selected chemical, physical and optical properties of oxyplumboroméite with other species of the roméite group.

Chemical composition

Eight electron microprobe analyses were obtained at different spots in the crystal used for crystal-structure refinements by wavelength dispersive spectroscopy using a Cameca SX50 instrument at the ''Istituto di Geologia Ambientale e Geoingegneria (Rome, Italy), CNR", operating at an acceleration voltage of 15 kV, a sample current of 15 nA and a 1 μm beam diameter. Minerals and synthetic standards used were InSb (Sb), wollastonite (Ca and Si), corundum (Al), magnetite (Fe), metallic manganese (Mn), celestine (Sr), baryte (Ba), galena (Pb and S) and jadeite (Na). The analyses were subject to ZAF corrections using the PAP routine (Pouchou and Pichoir, 1991). Elements with atomic numbers greater than 8, other than those listed, were below detection limits. Mean values, ranges and standard deviations of the analyses are summarized in Table 2.

The oxidation state of Fe was determined by ^{57}Fe Mössbauer spectroscopy at room temperature using a conventional spectrometer system operating in constant-acceleration mode. The spectrum was acquired by positioning a mineral powder absorber close to a ^{57}Co point-source in a rhodium matrix with a nominal activity of 10 mCi. The spectrum was calibrated against α-Fe foil and folded before fitting using the MDA software by Jernberg and Sundqvist (1983). The recorded spectrum shows a symmetric absorption doublet that is characterized by a small bandwidth of 0.28 mm/s (Fig. 2). Consequently, the spectrum could be fitted successfully using only one quadrupole doublet.

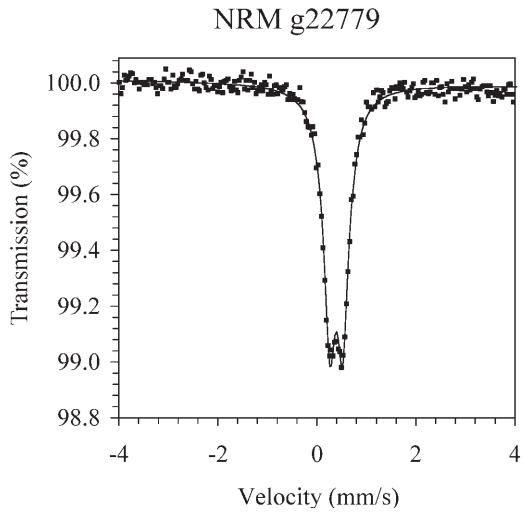

FIG. 2. Room-temperature ^{57}Fe Mössbauer spectrum of oxyplumboroméite (filled squares) and the fitted quadrupole doublet (solid line) caused by resonance absorption from Fe^{3+} at the B site.

TABLE 2. Chemical composition of oxyplumboroméite.

Constituent	Wt.% (mean)	Range	Stand. dev.
Sb_2O_5	48.69	48.30–49.20	0.31
SiO_2	0.00	0.00–0.02	0.01
Al_2O_3	0.01	0.00–0.03	0.01
Fe_2O_3[a]	3.85	3.74–4.05	0.10
CaO	8.46	8.39–8.58	0.05
MnO[b]	1.06	0.92–1.19	0.09
SrO	0.23	0.18–0.31	0.04
BaO	0.01	0.00–0.08	0.03
PbO	35.82	35.33–36.55	0.58
Na_2O	0.24	0.19–0.32	0.04
SO_3	0.07	0.02–0.10	0.03
H_2O[c]	0.05		
Total	98.49		
Atoms on the basis of 2 *B* cations p.f.u.			
Sb^{5+}	1.73		
Fe^{3+}	0.27		
Ca	0.87		
Mn	0.09		
Sr	0.01		
Pb	0.92		
Na	0.05		
OH	0.03		

[a] Based on Mössbauer spectroscopy results, iron is reported as Fe_2O_3
[b] Based on electronic absorption spectra, Mn is given as MnO
[c] H_2O content from single-crystal FTIR spectroscopy

The centre shift (CS) and quadrupole splitting (QS) parameters of this doublet, 0.39 and 0.25 mm/s, respectively, clearly demonstrates that iron is present as Fe^{3+} in a MO_6-polyhedron that is negligibly distorted from O_h symmetry.

Unpolarized FTIR spectra were collected at room temperature in transmission mode in the spectral range 2000−5000 cm^{-1} on a 49 μm thick doubly polished single crystal during 256 cycles using a square-shaped ~80 μm × 80 μm aperture at a nominal spectral resolution of 2 cm^{-1} with a Bruker Equinox 55S FTIR microscope spectrometer equipped with a glowbar source, KBr beamsplitter and MCT-detector. The recorded spectrum was fitted using the peak resolution program *Jandel PeakFit 4.12* assuming Gaussian lineshapes. The spectrum shows a set of five (OH) stretching bands in the 3400−3700 cm^{-1} spectral range (Fig. 3). No absorption bands in addition to these were observed in the measured IR spectral range. Peak positions of the observed (OH) stretching bands are 3613, 3571, 3547, 3527 and 3486 cm^{-1}. Using the spectrum evaluation method and calibration of Libowitzky and Rossman (1997), the content of $(OH)^-$ groups in the studied sample is determined from the FTIR spectrum to correspond to 0.05 wt.% H_2O.

An unpolarized room-temperature optical absorption spectrum (Fig. 4) was recorded on a 140 μm thick doubly-sided polished crystal platelet in the range 270−1100 nm (37037−9091 cm^{-1}) at a resolution of 1 nm using an AVASPEC-ULS2048X16 spectrometer attached *via* a 400 μm UV optical fibre to a Zeiss Axiotron UV-microscope. A 75W Xenon arc lamp served as illuminating source and Zeiss Ultrafluar 10× lenses served as objective and condenser. The circular measure aperture was 64 μm in diameter. The wavelength scale of the spectrometer was calibrated against Ho_2O_3-doped and Pr_2O_3/Nd_2O_3-doped standards (Hellma glass filters 666F1 and 666F7) with an accuracy better than 15 cm^{-1} in the wavelength range 300−1100 nm. The recorded spectrum shows a

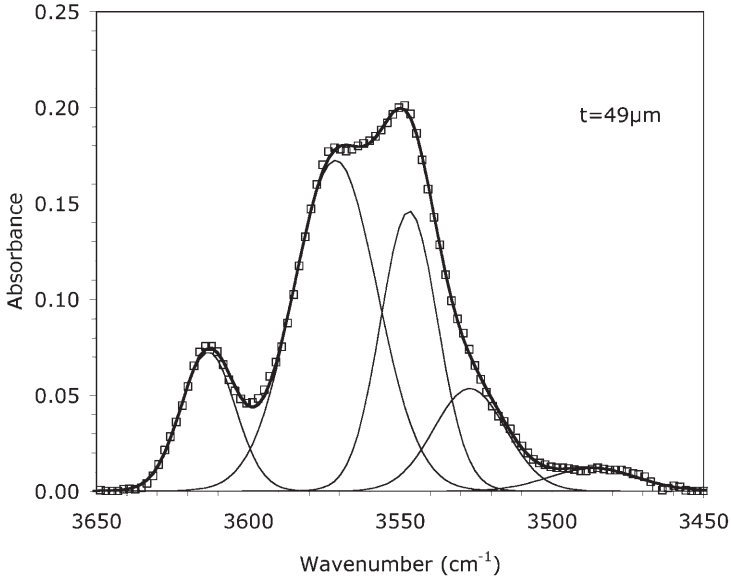

FIG. 3. Single-crystal FTIR spectrum of oxyplumboroméite in the (OH)-stretching region. Open squares show the measured spectrum, thin lines illustrate fitted individual (OH)-stretching bands and the thick line shows the resulting fitted total spectrum.

steep UV absorption caused by a band gap at ~21000 cm^{-1} (~2.60 eV). The brownish yellow colour of oxyplumboroméite is explained by the fact that the band gap effectively blocks transmission of the blue and violet components of visible light. The absence of intense and broad absorption bands in the UV/VIS/NIR spectral region furthermore demonstrates that the fraction of trivalent manganese is negligible in oxyplumboroméite. Consequently, the detected Mn contents are exclusively assigned to Mn^{2+}.

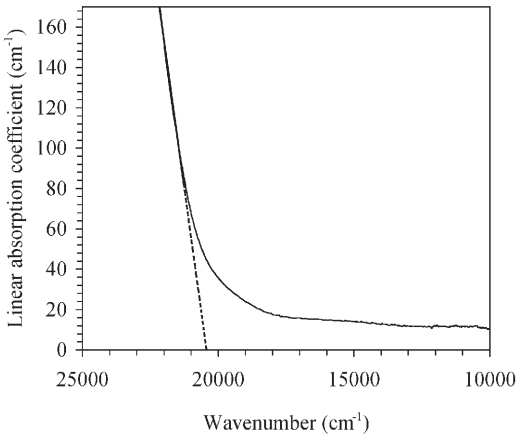

FIG. 4. Room-temperature optical absorption spectrum of a 140 µm thick single crystal of oxyplumboroméite (solid line) with the band gap energy indicated by the broken line.

Calculations on the basis of 2 *B* cations per formula unit, as recommended by Atencio *et al.* (2010), using the electron microprobe analyses in combination with the results from crystal-structure refinement, FTIR, Mössbauer and electronic absorption spectroscopy resulted in the empirical formula $^{A}(Pb_{0.92}Ca_{0.87}Mn_{0.09}Sr_{0.01}Na_{0.05})_{\Sigma 1.93}{}^{B}(Sb_{1.73}Fe^{3+}_{0.27})_{\Sigma 2.00}{}^{X+Y}[O_{6.64}(OH)_{0.03}]_{\Sigma 6.67}$, which leads to the endmember formula $Pb_2Sb_2O_7$. Oxyplumboroméite is the Pb analogue of oxycalcioroméite, ideally $Ca_2Sb_2O_7$ (Biagioni and Orlandi, 2012).

Crystal structure

The X-ray powder diffraction pattern was collected using a Panalytical X'pert powder diffractometer equipped with an X'celerator silicon-strip detector. The range 10–120º (2θ) was scanned with a step-size of 0.008º using a sample spinner with the sample mounted on a background-free holder. The diffraction data (in Å for CuKα, $\lambda\alpha_1$ = 1.54060 Å), corrected using Si as an internal standard, are listed in Table 3 together

TABLE 3. X-ray powder diffraction data for oxyplumboroméite.

I_{obs} (%)	I_{calc} (%)	d_{obs} (Å)	d_{calc} (Å)	h	k	l
100	**100**	2.9915	2.9949	2	2	2
32	**33**	2.5928	2.5937	4	0	0
2	1	2.3806	2.3801	3	3	1
48	**41**	1.8332	1.8340	4	4	0
38	**37**	1.5638	1.5640	6	2	2
11	9	1.4977	1.4975	4	4	4
5	5	1.2967	1.2968	8	0	0
12	**13**	1.1900	1.1901	6	6	2
9	11	1.1600	1.1599	8	4	0
8	7	1.0591	1.0589	8	4	4

Bold: five strongest diffraction lines

with calculated d and I values. Refined cell parameters from the powder diffraction data, using the program *UNITCELL* (Holland and Redfern, 1997), are: a = 10.3746(2) Å, V = 1117.65 (7) Å^3.

A representative crystal from the holotype specimen was selected for X-ray diffraction measurements on a Bruker KAPPA APEX-II single-crystal diffractometer, at the Sapienza University of Rome (Earth Sciences Department), equipped with a CCD area detector (6.2 cm × 6.2 cm active detection area, 512 × 512 pixels) and a graphite crystal monochromator, using Mo$K\alpha$ radiation from a fine-focus sealed X-ray tube. The sample-to-detector distance was 4 cm. A total of 1716 exposures (step = 0.2º,

TABLE 4. Single-crystal X-ray diffraction data details for oxyplumboroméite.

Temperature (K)	293(2)
Crystal colour	brownish yellow
Crystal size (mm)	0.20 × 0.22 × 0.28
Crystal system	Cubic
Space group	$Fd\bar{3}m$ (no. 227)
Unit-cell dimension a	10.3783(6) Å
Unit-cell volume V	1117.84(11) Å^3
Z	8
Density (calculated)	6.732 g/cm^3
Absorption coefficient (mm^{-1})	38.556
Axis, frame width (º), time per frame (s)	Phi-omega, 0.2, 20
Radiation, wavelength (Å)	Mo$K\alpha$, 0.71073
Range for data collection, 2θ (º)	6–73
Reciprocal space range *hkl*	$-7 \leqslant h \leqslant 16$; $-13 \leqslant k \leqslant 17$; $-14 \leqslant l \leqslant 13$
Total number of frames	1716
Set of read reflections	2494
Unique reflections, R_{int} (%)	160, 5.61
Redundancy	14
Absorption correction method	Multiscan (SADABS)
Refinement method	Full-matrix last-squares on F^2
Structural refinement program	*SHELXL-97*
Extinction coefficient	0.0088(8)
w$R2$ (%)	9.04
$R1$ (%) all data	3.02
$R1$ (%) for $I > 2\sigma_I$	2.98
GooF	1.366

TABLE 5. Fractional atomic coordinates and site occupancies for oxyplumboroméite.

Site	*x*	*y*	*z*	Site occupancy
A	0.500	0.500	0.500	$Pb_{0.524(5)}Ca_{0.476(5)}$
B	0.000	0.000	0.000	$Sb_{1.00}$
O1($\equiv X$)	0.3228(5)	0.125	0.125	$O_{1.00}$
O2($\equiv Y$)	0.375	0.375	0.375	$O_{1.00}$

time/step = 20 s) covering a full reciprocal sphere with a redundancy of 14 was used. Final unit-cell parameters were refined by means of the Bruker AXS *SAINT* program using reflections with $I > 10\ \sigma(I)$ in the range $5° < 2\theta < 73°$. The intensity data were processed and corrected for Lorentz, polarization and background effects with the *APEX2* software program of Bruker AXS. The data were corrected for absorption using the multi-scan method (SADABS). The absorption correction led to a significant improvement in R_{int}. No violations of $Fd\bar{3}m$ symmetry were noted.

Structural refinement was done with the *SHELXL-97* program (Sheldrick, 2008). Variable parameters were: scale factor, extinction coefficient, atomic coordinates, site scattering values and atomic displacement factors. To obtain the best values of statistical indexes ($R1$, $wR2$), a fully ionized scattering curve for O was used, whereas neutral scattering curves were used for the other atoms. In detail, the occupancy of the *A* site was modelled by using Pb and Ca scattering factors, and the *B* site using Sb scattering factor. Three full-matrix refinement cycles with isotropic displacement parameters for all atoms were followed by anisotropic cycles until convergence was attained. No significant correlations over a value of 0.7 between the parameters were observed at the end of the refinement. Table 4 lists crystal data, data collection information and refinement details; Table 5 gives the fractional atomic coordinates and site occupancies; Table 6 gives the displacement parameters; Table 7 summarizes selected bond distances.

The crystal structure of oxyplumboroméite is characterized by corner-sharing BO_6 octahedra forming the typical pyrochlore framework (Fig. 5). The eight-coordinated *A* site is preferentially occupied by Pb and to a lesser degree by Ca. The Pb/Ca occupancy ratio obtained from the crystal structure refinement of 1.10 is in good agreement with the ratio of 1.09 recorded by the electron microprobe analyses. The bond-valence analysis is consistent with the empirical structural formula. Bond-valence calculations, using the formula and bond-valence parameters from Brown and Altermatt (1985), Krivovichev and Brown (2001) for Pb^{2+} and Mills *et al*. (2009) for Sb^{5+}, show that the bond valence sums at the cation sites (A = 2.30 valence unit (vu) and B = 4.74 vu) are consistent with the presence of divalent cations at *A* and pentavalent and trivalent cations at *B*, while the bond valence sums at the anion sites (X = 2.02 vu and Y = 2.00 vu) are consistent with occupancy by O^{2-}. Crystal-structure analysis shows large displacement parameters for the *A* and *Y* sites, ~0.02 $Å^2$ and 0.03 $Å^2$, respectively, indicating static positional disorder in the oxyplumboroméite structure. Moreover, the somewhat larger bond-valence sum incident at the *A* site (2.30 vu compared to an expected value of 2 vu), indicates the

TABLE 6. Displacement parameters ($Å^2$) for oxyplumboroméite.

Site	U^{11}	U^{22}	U^{33}	U^{23}	U^{13}	U^{12}	U_{eq}
A	0.0190(5)	0.0190(5)	0.0190(5)	–0.00324(13)	–0.00324(13)	–0.00324(13)	0.0190(5)
B	0.0083(4)	0.0083(4)	0.0083(4)	–0.00065(10)	–0.00065(10)	–0.00065(10)	0.0083(4)
O1 ($\equiv X$)	0.011(2)	0.0091(12)	0.0091(12)	0.0043(15)	0	0	0.0096(10)
O2 ($\equiv Y$)	0.030(4)	0.030(4)	0.030(4)	0	0	0	0.030(4)

Equivalent (U_{eq}) displacement parameters.

TABLE 7. Relevant bond distances (Å) for oxyplumboroméite.

A–O1 (×6)	2.597(3)	*B*–O1 (×6)	1.9843(18)
A–O2 (×2)	2.2470(1)		
<*A*–O>	2.510		

occurrence of bond strain, probably because the dominant *A*-site cation, Pb^{2+}, is located in a cavity that is too small (e.g. Brown, 2009). The static disorder connected with the *A* site is probably related to the stereoactive lone-pair electronic configuration of Pb^{2+}. Comparable effects have been noted in a wide range of pyrochlore-type compounds with *A* cations of lone-pair character, as, for instance, in the cubic phase $Bi_2Ti_2O_7$ (Hector and Wiggin, 2004).

A comment on the identification of bindheimite

In their chemical and powder X-ray study on antimony oxides and antimonates, Mason and Vitaliano (1953) examined specimens of bindheimite from Lovelock, Nevada, USA, San Bernadino County, California, USA and one specimen of "monimolite" from the Harstigen mine (evidently one of the samples used by Flink (1887) in his study of "monimolite"). Mason and Vitaliano (1953) concluded that the powder X-ray patterns of bindheimeite and "monimolite" were almost identical. However, in contrast to the analysis of "monimolite", in which they detected no water, they analysed 5.04–5.78 wt.% H_2O in their bindheimite samples. Furthermore, they obtained considerably larger values for the density and the refractive index of "monimolite" (7.29 g cm^{-3} and >2.06, respectively) as compared to bindheimite (5.16–5.28 g cm^{-3} and 1.905–1.928, respectively). Based on the results of their study, it seems reasonable to assume that some "bindheimite" samples may in fact represent a possible new species "hydroxyplumboroméite". Consequently, the suggestion that bindheimite is identical to oxyplumboroméite (Atencio *et al.*,

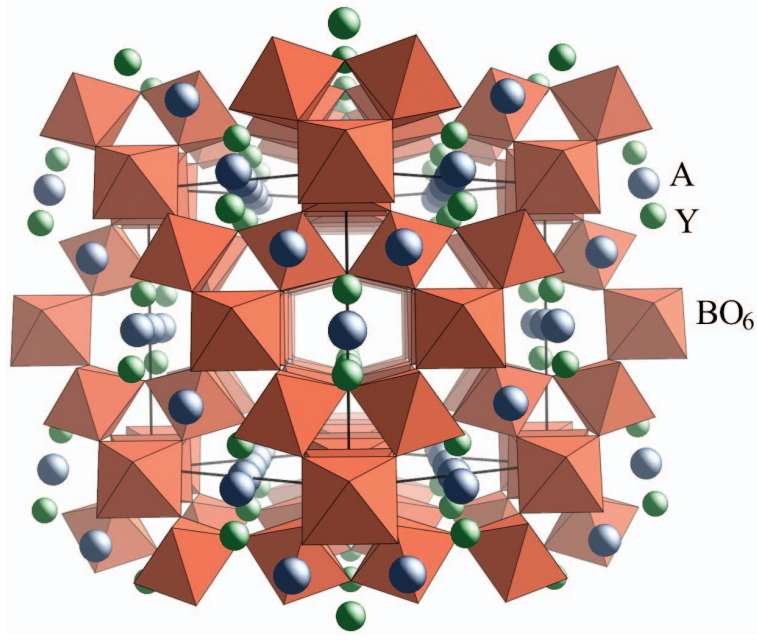

FIG. 5. The crystal structure of oxyplumboroméite looking down [101]. [BO_6] octahedra are shown in brown. Circles filled with grey and green correspond to A and Y atoms, respectively.

2010; Christy and Atencio, 2013) may not generally apply. Further chemical and structural examination of bindheimite is evidently needed.

Acknowledgements

Chemical analyses were carried out with the kind assistance of M. Serracino to whom we express our gratitude. The reviewers Andrew Christy, Daniel Atencio and Peter Leverett are thanked for helpful suggestions and comments. We appreciate the efficient handling of the manuscript by Peter Williams (Principal Editor) and Andrew Christy (Associate Editor).

References

Arents, A. (1867) Partzite, a new mineral. *American Journal of Science*, **93**, 362.

Atencio, D., Andrade, M.B., Christy, A.G., Gieré, R. and Kartashov, P.M. (2010) The pyrochlore supergroup of minerals: nomenclature. *The Canadian Mineralogist*, **48**, 673–698.

Atencio, D., Ciriotti, M.E. and Andrade, M.B. (2013) Fluorcalcioroméite, $(Ca,Na)_2Sb_2^{5+}(O,OH)_6F$, a new roméite-group mineral from Starlera mine, Ferrera, Grischun, Switzerland: description and crystal structure. *Mineralogical Magazine*, **77**, 467–473.

Beudant, F.S. (1837) *Traité élémentaire de Minéralogie (deuxième édition)*. Carilian Jeune, Libraire, Paris, France.

Biagioni, C. and Orlandi, P. (2012) Oxycalcioroméite, IMA2012-022. CNMNC Newsletter No. 14, October 2012, page 1283; *Mineralogical Magazine*, **76**, 1281–1288.

Brown, I.D. (2009) Recent developments in the methods and applications of the bond valence model. *Chemical Reviews*, **109**, 6858–6919.

Brown, I.D. and Altermatt, D. (1985) Bond-valence parameters obtained from a systematic analysis of the inorganic crystal structure database. *Acta Crystallographica*, **B41**, 244–247.

Brugger, J., Gieré, R.R., Graeser, S. and Meisser, N.N. (1997) The crystal chemistry of roméite. *Contributions to Mineralogy and Petrology*, **127**, 136–146.

Christy, A.G. and Atencio, D. (2013) Clarification of status of species in the pyrochlore supergroup. *Mineralogical Magazine*, **77**, 13–20.

Christy, A.G. and Gatedal, K. (2005) Extremely Pb-rich rock-forming silicates including a beryllian scapolite and associated minerals in a skarn from Långban, Värmland, Sweden. *Mineralogical Magazine*, **69**, 995–1018.

Flink, G. (1887) Mineralogiska notiser I.7. Monimolit från Pajsberg. *Bihang till Kongliga Vetenskapsakademiens Handlingar*, **12**, 35–40.

Hector, A.L. and Wiggin, S.B. (2004) Synthesis and structural study of stoichiometric $Bi_2Ti_2O_7$ pyrochlore. *Journal of Solid State Chemistry*, **177**, 139–145.

Holland, T.J.B. and Redfern, S.A.T. (1997) Unit cell refinement from powder diffraction data: the use of regression diagnostics. *Mineralogical Magazine*, **61**, 65–77.

Hussak, E.E. and Prior, G.T. (1895) Lewisite and zirkelite, two new Brazilian minerals. *Mineralogical Magazine*, **11**, 80–88.

Igelström, L.J. (1865) Nya och sällsynta mineralier från Vermland. *Öfversigt af Kongl. Vetenskaps-Akademiens Förhandlingar*, **22**, 227–229.

Jernberg, P. and Sundqvist, T. (1983) A versatile Mössbauer analysis program. Uppsala University, Institute of Physics (UUIP-1090).451

Libowitzky, E. and Rossman, G.R. (1997) An IR absorption calibration for water in minerals. *American Mineralogist*, **82**, 1111–1115.

Krivovichev and Brown (2001) Are the compressive effects of encapsulation an artifact of the bond valence parameters? *Zeitschrift fur Kristallographie*, **216**, 245–247.

Mandarino, J.A. (1979) The Gladstone-Dale relationship. Part III. Some general applications. *The Canadian Mineralogist*, **17**, 71–76.

Mandarino, J.A. (1981) The Gladstone-Dale relationship. Part IV. The compatibility concept and its application. *The Canadian Mineralogist*, **19**, 441–450.

Mason, B. and Vitaliano, C.J. (1953) The mineralogy of the antimony oxides and antimonates. *Mineralogical Magazine*, **30**, 100–112.

Matsubara, S., Kato, A.A., Shimizu, M., Sekiuchi, K. and Suzuki, Y. (1996) Romeite from Gozaisho mine, Iwaki, Japan. *Mineralogical Journal*, **18(4)**, 155–160.

Mills, S.J., Christy, A.G., Chen, E.C.-C. and Raudsepp, M. (2009) Revised values of the bond valence parameters for $^{[6]}$Sb(V)-O and $^{[3-11]}$Sb(III)-O. *Zeitschrift fur Kristallographie*, **224**, 423–431.

Pouchou, J.L. and Pichoir, F. (1991) Quantitative analysis of homogeneous or stratified microvolumes applying the model "PAP". Pp. 31–75 in: *Electron Probe Quantitation* (K.F.J. Heinrich and D.E. Newbury, editors). Plenum, New York.

Riotte, E.N. (1867) Stetefeldtit, ein neues Mineral. *Berg- und Huettenmännische Zeitung*, **26**, 253–254.

Sheldrick, G.M. (2008) A short history of SHELX. *Acta Crystallographica*, **A64**, 112–122.

Walenta, K. (1983) Bismutostibiconit, ein neues Mineral der Stibiconitgruppe aus dem Schwarzwald. *Chemie der Erde*, **42**, 77–81.